euronoise

FE-Model Reduction for FE-BE Coupling with Large Fluid-Structure Interfaces

Michael Junge, Jens Becker, Dominik Brunner and Lothar Gaul

Institute of Applied and Experimental Mechanics, University of Stuttgart, Pfaffenwaldring 9, 70550 Stuttgart, Germany
junge@iam.uni-stuttgart.de

For the finite element method, reduction techniques exist to represent the dynamic behavior of component substructures. The reduction basis of both the Craig-Bampton method and the Rubin method contain component modes, which are computed for all structural degrees of freedom on an interface. The interface can either be defined by adjacent substructures or by coupling interfaces to other physical domains, as it is the case for FE-BE coupled systems. A large interface thus leads to an increased size of the reduced order model and limits standard model reduction techniques to applications with small interfaces. In this work, interface reduction methods are investigated, enabling an efficient solution of the vibro-acoustic behavior of fluid-structure coupled systems. Here, the size of the reduced order model is decreased by reducing the number of retained interface modes, while marginally increasing the reduction error. A direct reduction method based on strain–energy considerations is presented. Additionally, an iterative reduction scheme is proposed which only adds a basis vector to the reduction basis, if the spanned subspace is sufficiently enlarged. The applicability of the proposed methods is shown for an example structure.

1 Introduction

The vibro-acoustic behavior of thin structures is significantly altered if they are partly immersed or totally submerged in water. A strong fluid-structure interaction is observed and the structural problem (domain Ω_s in Fig. 1) and acoustic problem (Ω_a) can no longer be solved separately. A strong coupling scheme has to be applied, where the feedback of the hydraulic pressure onto the structure at the fluid-structure interface Γ_i is not neglected. The finite element method (FEM) is widely used to simulate the dynamic behavior of structures. The boundary element method (BEM) shows its strength for the solution of the exterior acoustic problem, since its fundamental solution intrinsically fulfills the Sommerfeld radiation condition. In [1] a fully coupled FE-BE formulation is investigated and different solver strategies for an efficient solution of large-scale systems are discussed. For large structural problems, the treatment of the FE-part is expensive and in the low-frequency regime may be a dominant part of the solution process. Component mode synthesis (CMS) methods exist, such as the Craig-Bampton method and the Rubin method [2] which accelerate pure FE frequency sweep computations. In case of FE-BE coupling the size of the fluid-structure interface has a direct influence on the size of the reduced-order model. This limits the use of these CMS methods to systems with a small coupling interface. For this reason interface reduction methods (IR-methods) are developed, which significantly broadens the range of use of CMS-methods [3].

This work focuses on FE interface reduction techniques for the efficient solution of strongly coupled FE-BE simulations and is organized as follows: First the FE-BE coupled formulation is briefly presented. Then, then the Craig-Bampton method and the Rubin method are reviewed, which provides the basis for the subsequent IR-methods. Two IR-methods, one for the Craig-Bampton method and one for the Rubin method, are presented. The reduction methods are applied to predict the vibro-acoustic behavior of a partly submerged semi-ellipsoid test structure and compared with respect to their accuracy and computation time to the full-order solution.

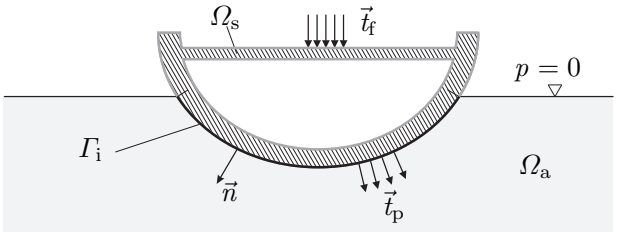

Figure 1: Domains of the coupled problem. The exterior acoustic domain Ω_a is in contact with the structure Ω_s on the fluid–structure interface Γ_i. The stress vectors are denoted by $\vec{t}_\mathrm{f}$ and $\vec{t}_\mathrm{p}$.

2 FE-BE coupled formulation

With the time-harmonic behavior $\mathrm{e}^{-\mathrm{j}\omega t}$, the FE-formulation in the structural domain Ω_s reads

$$\underbrace{\left(-\omega^2\mathbf{M} - \mathrm{j}\omega\mathbf{D} + \mathbf{K}\right)}_{\mathbf{K}_\mathrm{FE}}\mathbf{u} = -\mathbf{C}_\mathrm{FE}\,\mathbf{p} + \mathbf{f}\,, \qquad (1)$$

where ω is the angular excitation frequency and j denotes the imaginary unit. In Eq (1), $\mathbf{K}$ and $\mathbf{M}$ are the stiffness matrix and mass matrix, respectively. The nodal displacement vector is given by $\mathbf{u}$ ($\in \mathbb{R}^{N_\mathrm{s}}$) and $\mathbf{f}$ ($\in \mathbb{R}^{N_\mathrm{s}}$) denotes the nodal force vector. The acoustic pressure $\mathbf{p}$ ($\in \mathbb{R}^{N_\mathrm{I}}$) is coupled to the structure via the coupling matrix $\mathbf{C}_\mathrm{FE}$. Hereby, N_s and N_I are the number of degrees of freedom (DOF) of the whole structure and of the fluid–structure interface, respectively. In this work, structural damping is modeled by Rayleigh damping $\mathbf{D} = \alpha\mathbf{M}+\beta\mathbf{K}$. Since water is nearly incompressible, the fluid formulation starts with the Laplace equation [4]

$$\Delta^2 p(\vec{x}) = 0 \quad \text{for} \quad \vec{x} \in \Omega_\mathrm{a}\,, \qquad (2)$$

where p denotes the pressure and the Laplacian is given by Δ^2. The Laplace equation is valid for the pressure p at an arbitrary point $\vec{x}$ within the exterior acoustic domain Ω_a (cf. Fig. 1) for an incompressible fluid. A weak form of the Laplace equation is obtained by weighting with the fundamental solution

$$P(\vec{x},\vec{y}) = \frac{1}{4\,\pi\,r} - \frac{1}{4\,\pi\,r'}\,, \qquad (3)$$

where $r = |\vec{x} - \vec{y}|$ denotes the distance between the load and the field point. The second term in (3) accounts for the pressure-free boundary condition of the water surface [5, 6]. Therefore, x is mirrored on the water surface. The distance between the mirrored point x' and the point y is given by $r' = |\vec{x}' - \vec{y}|$. Applying Green's

second theorem yields the representation formula, which is valid for any $\vec{x}$ in the acoustic domain Ω_a. The hypersingular boundary integral equation is obtained from the representation formula and reads

$$\frac{1}{2}q(\vec{x}) = -\underbrace{\int_{\Gamma_\mathrm{i}} \frac{\partial P(\vec{x},\vec{y})}{\partial \vec{n}_x}\, q(\vec{y})\,\mathrm{d}s_y}_{(K'q)(\vec{x})} + \underbrace{\int_{\Gamma_\mathrm{i}} \frac{\partial^2 P(\vec{x},\vec{y})}{\partial \vec{n}_x \partial \vec{n}_y}\, p(\vec{y})\,\mathrm{d}s_y}_{-(Dp)(\vec{x})}\,, \tag{4}$$

where K' denotes the adjoint double layer potential and D is the hypersingular operator. The variable q represents the acoustic flux, which is defined on Γ_i as $q(\vec{x}) := {}^{\partial p(\vec{x})}/_{\partial \vec{n}_x}$. To obtain an algebraic system of equations from Eq (4), the boundary Γ_i is discretized. The BE-formulation for the acoustic fluid then reads

$$\mathbf{K}_\mathrm{BE}\,\mathbf{p} - \underbrace{(\mathbf{I} - \mathbf{K}')}_{\mathbf{C}^q_\mathbf{BE}}\mathbf{q} = 0\,. \tag{5}$$

Hereby, the Galerkin matrices $\mathbf{K}_\mathrm{BE}$ and $\mathbf{K}'$ correspond to the hypersingular operator and the adjoint double layer potential, respectively. In order to obtain a FE-BE coupled formulation a relation between the acoustic flux $q(\vec{y})$ and the particle displacement $\vec{u}_\mathrm{f}(\vec{y})$ is established using Euler's equation. For triangular elements it reads

$$q^{(\mathrm{e})} = \frac{1}{3}\varrho_\mathrm{f}\omega^2 \sum_{\mathrm{k}\in\mathrm{e}} u^\mathrm{k}_{\vec{n}}\,, \tag{6}$$

where the variable k loops over all vertices of the selected element e. The transformation is written in matrix notation as $\mathbf{q} = \mathbf{T}_\mathrm{q}\mathbf{u}$ where $\mathbf{q}$ denotes the vector with the flux on the elements. The matrix $\mathbf{T}_q$ selects only displacements of translational DOFs on Γ_i. By using this relation and Eqs. (1) and (5) the fully-coupled Schur-complement system reads

$$\underbrace{\left(\mathbf{K}_\mathrm{BE} - \mathbf{C}^q_\mathrm{BE}\mathbf{T}_q\mathbf{K}^{-1}_\mathrm{FE}\mathbf{C}_\mathrm{FE}\right)}_{\mathbf{S}}\mathbf{p} = -\mathbf{C}^q_\mathrm{BE}\mathbf{T}_q\mathbf{K}^{-1}_\mathrm{FE}\mathbf{f}\,, \tag{7}$$

with the vector of unknowns $\mathbf{p}$ and the Schur complement $\mathbf{S}$. A single GMRES is directly applied for $\mathbf{S}$, with a simple diagonal scaling as a preconditioner for $\mathbf{K}_\mathrm{BE}$. This solution strategy turned out to be efficient [1]. To speed up the solution process FE model reduction techniques shall now be applied for a faster factorization of $\mathbf{K}_\mathrm{FE}$, which is needed for the solution of Eq. (7).

3 Model Order Reduction

Both the Craig-Bampton method and the Rubin method are based on a consistent Rayleigh-Ritz coordinate transformation

$$\mathbf{u} = \mathbf{\Theta}\,\mathbf{z}\,, \tag{8}$$

where $\mathbf{z}$ denotes the generalized coordinates and $\mathbf{\Theta}$ is a coordinate transformation matrix of component modes. By left-multiplication of Eq. (1) with $\mathbf{\Theta}^\mathrm{T}$ and making use of Eq. (8), Eq. 1 is expressed in generalized coordinates

$$\underbrace{\left(-\omega^2\tilde{\mathbf{M}} - \mathrm{j}\omega\tilde{\mathbf{D}} + \tilde{\mathbf{K}}\right)}_{\tilde{\mathbf{K}}_\mathrm{FE}}\mathbf{z} = -\mathbf{\Theta}^\mathrm{T}\mathbf{C}_\mathrm{FE}\,\mathbf{p} + \tilde{\mathbf{f}}_\mathrm{s}\,, \tag{9}$$

where $\tilde{\mathbf{M}} = \mathbf{\Theta}^\mathrm{T}\mathbf{M}\mathbf{\Theta}$, $\tilde{\mathbf{K}} = \mathbf{\Theta}^\mathrm{T}\mathbf{K}\mathbf{\Theta}$, and $\tilde{\mathbf{f}} = \mathbf{\Theta}^\mathrm{T}\mathbf{f}$ are the reduced mass matrix, stiffness matrix and the load vector in the generalized coordinate system, respectively. In contrast to the sparse matrices $\mathbf{M}$ and $\mathbf{K}$, the dense matrices $\tilde{\mathbf{M}}$ and $\tilde{\mathbf{K}}$ are fully populated. The Schur complement formulation analogue to (7) then reads

$$\left(\mathbf{K}_\mathrm{BE} - \mathbf{C}^q_\mathrm{BE}\mathbf{T}_q\mathbf{\Theta}\tilde{\mathbf{K}}^{-1}_\mathrm{FE}\mathbf{\Theta}^\mathrm{T}\mathbf{C}_\mathrm{FE}\right)\mathbf{p} = -\mathbf{C}^q_\mathrm{BE}\mathbf{T}_u\mathbf{\Theta}\tilde{\mathbf{K}}^{-1}_\mathrm{FE}\mathbf{\Theta}^\mathrm{T}\mathbf{f}\,. \tag{10}$$

Without loss of generality, it will be assumed in the following that $\mathbf{M}$ and $\mathbf{K}$ in Eq. (1) are partitioned as

$$\begin{bmatrix}\mathbf{M}_\mathrm{II} & \mathbf{M}_\mathrm{IF}\\ \mathbf{M}_\mathrm{FI} & \mathbf{M}_\mathrm{FF}\end{bmatrix}\begin{bmatrix}\ddot{\mathbf{u}}_\mathrm{I}\\ \ddot{\mathbf{u}}_\mathrm{F}\end{bmatrix} + \begin{bmatrix}\mathbf{K}_\mathrm{II} & \mathbf{K}_\mathrm{IF}\\ \mathbf{K}_\mathrm{FI} & \mathbf{K}_\mathrm{FF}\end{bmatrix}\begin{bmatrix}\mathbf{u}_\mathrm{I}\\ \mathbf{u}_\mathrm{F}\end{bmatrix} = \begin{bmatrix}\mathbf{f}_\mathrm{I}\\ \mathbf{f}_\mathrm{F}\end{bmatrix}\,, \tag{11}$$

where $\mathbf{u}_\mathrm{I}$ contains displacements of all DOFs, which are located on the FE-BE interface Γ_i, while $\mathbf{u}_\mathrm{F}$ contains all displacements of free (or inner) DOFs. The vectors $\mathbf{u}_\mathrm{I}$ and $\mathbf{u}_\mathrm{F}$ shall be of size N_I and N_F, respectively with $N_\mathrm{s} := N_\mathrm{I} + N_\mathrm{F}$.

Craig-Bampton and Rubin Method For the Craig-Bampton method the component mode matrix is populated by fixed-interface normal modes $\mathbf{\Phi}_\mathrm{CB}$ and by constraint modes $\mathbf{\Psi}_\mathrm{CB}$. The former are the $N^\mathbf{\Phi}_\mathrm{CB}$ lowest eigenvectors of the generalized hermitian eigenvalue problem obtained by fixing all interface DOFs

$$\left(-\omega^2_{\mathrm{CB}j}\,\mathbf{M}_\mathrm{FF} + \mathbf{K}_\mathrm{FF}\right)\hat{\mathbf{\Phi}}_{\mathrm{CB}j} = 0,\ j = 1, 2, \ldots, N^\mathbf{\Phi}_\mathrm{CB}\,. \tag{12}$$

The later are determined by fixing all but one interface DOFs and computing the static solution due to the unit deflection applied at the remaining unfixed interface DOFs. The coordinate transformation matrix is thus given by

$$\mathbf{\Theta}_\mathrm{CB} = \begin{bmatrix}\mathbf{\Psi}_\mathrm{CB} & \mathbf{\Phi}_\mathrm{CB}\end{bmatrix} = \begin{bmatrix}\mathbf{I}_{N_\mathrm{I}} & \mathbf{0}\\ -\mathbf{K}^{-1}_\mathrm{FF}\mathbf{K}_\mathrm{FI} & \hat{\mathbf{\Phi}}_\mathrm{CB}\end{bmatrix} \tag{13}$$

In contrast to the Craig-Bampton method, the Rubin method is a free interface method, i.e. neither the interface DOFs nor the free DOFs are additionally constrained for the computation of the component modes in $\mathbf{\Theta}_\mathrm{Ru}$. The $N^\mathbf{\Phi}_\mathrm{Ru}$ free-interface normal modes $\mathbf{\Phi}_\mathrm{Ru}$ are computed by solving the eigenvalue problem of the unconstrained system. Attachment modes $\mathbf{\Psi}_\mathrm{Ru}$ augment the component modes matrix accounting for the modal truncation error. They are defined by the static solution vector due to a single unit force applied to one DOF on the interface. Attachment modes cannot be computed directly, if the structure has rigid-body degrees of freedom and thus rigid body modes $\mathbf{\Psi}_\mathrm{rb}$ ($\mathbf{\Psi}_\mathrm{rb} \in \mathbb{R}^{N_\mathrm{s}\times N_\mathrm{rb}}, 0 \le N_\mathrm{rb} \le 6$). Instead of the standard attachment modes, either inertia-relief attachment modes, residual flexibility attachment modes or shifted attachment modes are used [2]. In this work shifted attachment modes are employed. Thus, the transformation matrix is given by

$$\mathbf{\Theta}_\mathrm{Ru} = \begin{bmatrix}\mathbf{\Psi}_\mathrm{Ru\,sh} & \mathbf{\Phi}_\mathrm{Ru}\end{bmatrix}\,. \tag{14}$$

In both methods the size of the reduced order model is directly related to the size of the interface. In case of FE-BE coupling, where the fluid-structure interface may

contain several thousand interface DOFs, both methods no longer show a speedup comparing the solution time of the sparse full-size model and the dense reduced-order model.

3.1 IR-Methods

The key idea of the IR-methods is to find a dominant subspace of the static component modes $\mathbf{\Psi}_{\mathrm{CB}}$ and $\mathbf{\Psi}_{\mathrm{Ru}}$, respectively.

IR for the Craig-Bampton method In [3] it is suggested to find the dominant directions with respect to the **K**-norm. In contrast to the Euclidean norm, this norm accounts for the different scaling of translational and rotational DOFs and for inhomogeneities in stiffness and mass. The dominant directions are obtained by the solution of the generalized eigenvalue problem of the Guyan-reduced system

$$\mathbf{\Psi}_{\mathrm{CB}}^{\mathrm{T}}\mathbf{K}\mathbf{\Psi}_{\mathrm{CB}}\mathbf{\Upsilon}_{\mathrm{CB-ir}\,j} = \omega_{\mathrm{CB-ir}\,j}\mathbf{\Psi}_{\mathrm{CB}}^{\mathrm{T}}\mathbf{M}\mathbf{\Psi}_{\mathrm{CB}}\mathbf{\Upsilon}_{\mathrm{CB-ir}}\,. \tag{15}$$

The vectors $\mathbf{\Psi}_{\mathrm{CB}}\mathbf{\Upsilon}_{\mathrm{CB}\,1}$ represent the reduced interface modes. Since the interface modes with the lowest strain-energy are more likely to be exposed, only $N_{\mathrm{CB-ir}}$ modes are retained. This leads to the reduction basis for the Craig-Bampton method with interface reduction

$$\begin{bmatrix}\mathbf{u}_{\mathrm{I}}\\ \mathbf{u}_{\mathrm{F}}\end{bmatrix} = \underbrace{\begin{bmatrix}\mathbf{\Psi}_{\mathrm{CB}}\mathbf{\Upsilon}_{\mathrm{CB}\,1}\ldots\mathbf{\Psi}_{\mathrm{CB}}\mathbf{\Upsilon}_{\mathrm{CB}\,N_{\mathrm{CB-ir}}} & \mathbf{\Phi}_{\mathrm{CB}}\end{bmatrix}}_{\mathbf{\Theta}_{\mathrm{CB-ir}}}\begin{bmatrix}\boldsymbol{\eta}_{\mathrm{CB\,ir}}\\ \boldsymbol{\xi}_{\mathrm{CB}}\end{bmatrix}. \tag{16}$$

This method is denoted `CB-ir`. For fluid-structure coupling, the pressure always acts in the normal direction. Therefore, it is sufficient to use so-called normal constraint modes instead of the standard constraint modes. They are computed by applying a unit displacement constraint in the nodal normal direction, instead of unit displacement constraints in all global coordinate directions. This is realized by defining a local coordinate transformation for all nodes, such that one coordinate axis is parallel to the nodal normal vector. The in-plane DOFs as well as the rotational DOFs are then considered as free DOFs. By this, the size of the system in Eq. (15) is reduced to 1/6 of the original system if rotational DOFs are present on the interface, otherwise to 1/3. This modified method is denoted `CB-n-ir` for later use. Both methods `CB-ir` and `CB-n-ir` have in common, that the reduced subspace of $\mathbf{\Psi}_{\mathrm{CB}}$ is selected as dominant directions with respect to strain energy, thus fulfilling some sort of optimality. To find this subspace necessitates in a first step the computation of all constraint modes, leading to a high peak memory consumption for storing all constraint modes. In a second step, the memory consumption is then significantly reduced by the interface reduction. However, critically high peak values for the memory consumption might render the interface reduction impossible. This motivated the definition of an iterative interface reduction method in the next subsection, which shows lower memory peak values.

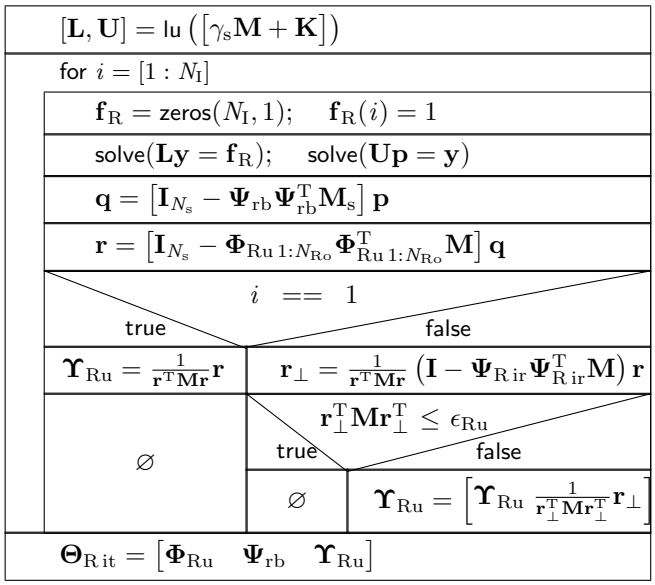

Figure 2: Structogramm of the method Ru-ir

IR for the Rubin Method When forming the inner product of two attachment modes located on adjacent nodes, a strong collinearity is observed. This collinearity is exploited by the iterative interface reduction scheme `Ru-ir`. A structogramm of it is depicted in Fig. 2. For every attachment mode it is checked, if its inclusion in the reduction basis significantly enlarges the range of the present reduction basis. If so, its **M**-orthogonal part is used to augment the reduction basis. If not, it is discarded. It is worth noting, that the attachment mode is orthogonalized to the rigid body modes $\mathbf{\Psi}_{\mathrm{rb}}$ and to the lowest N_{Ro} free-interface normal modes $\mathbf{\Phi}_{\mathrm{Ru}}$. The component mode basis of the method `Ru-ir` is then populated by the free-interface normal modes, rigid body modes and the matrix $\mathbf{\Upsilon}_{\mathrm{Ru}}$. If instead of the standard attachment modes, so-called normal attachment modes are used, the method is denoted `Ru-n-ir`.

4 Numerical example

In this section, the proposed methods are applied to a partly immersed example structure as depicted in Fig 3. One half of an ellipsoid forms the hull. It is covered by a curved cover plate. The ellipsoid has a length of 10.00 m, a width of 5.00 m and a total height of 3.75 m. The hull has a shell thickness of 0.05 m, the cover of 0.01 m. Steel (E=207 GPa, ν=0.3, ρ_{s}=7669 kg/m³) is used as material for the hull. Though not physically correct, the cover is modeled by a higher E-modulus, instead of modeling additionally stiffening elements. This keeps the model as simple as possible. The FE-model consists of 1484 shell elements width 1159 nodes, yielding 6954 DOFs (both translational and rotational). The commercial FE-package ANSYS is used to set up the FE-system using SHELL181 elements. The dark colored elements (308 elements) are in contact with water (ρ_{f}=1000 kg/m³). Rayleigh damping is assumed with the parameters $\alpha = 1.0$ 1/s and β=5.0×10^{-6} s. The system is completely unconstrained. Since a conforming

coupling scheme is applied, the BE-mesh is created directly from the FE-mesh. The system is excited by a nodal force in y-direction at point A, located on one symmetry axis on the cover as depicted in Fig. 3. The system behavior is investigated in a frequency range between 10 and 100 Hz with a step size of 0.5 Hz. The displacement in y-direction at point A is considered as an additional interface DOF and the corresponding constraint or attachment modes are always added to the reduction basis.

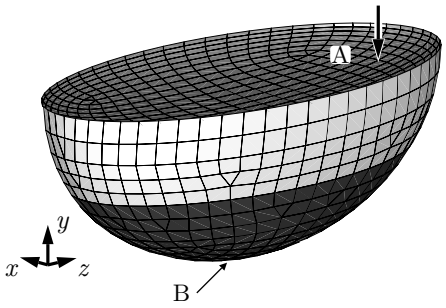

Figure 3: Partly immersed semi-ellipsoid test structure. The dark-colored elements are in contact with water. The structure is excited by a vertical force vector at node A. Response is calculated at node B.

For a better physical understanding of the reduction methods, Fig. 4 shows normal modes used for the Craig Bampton method and the method `CB-ir`. It can well be observed that all interface DOFs are fixed for the fixed-interface normal modes (cf. Fig. 4(a)) and all but one interface DOFs are fixed for the depicted constraint mode (cf. Fig. 4(b)). This is not the case for the reduced interface modes (Figs. 4(c) and 4(d)), which instead of the fixed-interface normal modes are used for the method `CB-ir` and `CB-n-ir`. Analogue to Fig. 4 the contour plots in Fig. 5(a) shows one attachment mode as it used used for the Rubin method. The white colored spots in Fig. 5(b) mark the nodes, of which the m-orthogonal part of the normal attachment modes is retained in the reduction basis $\boldsymbol{\Upsilon}_{\mathrm{Ru}}$ for one of the models obtained by the method `Ru-n-ir`. Since the structure processes an evenly distributed density and a similar stiffness on the interface the selected attachment are also geometrically distributed evenly.

The upper plot of Fig. 6 shows the dynamic compliance frequency response function (FRF) for the given input at node A to the displacement in y-direction at node B, H_{AB}, for various models obtained by the interface reduction methods `CB-ir` and `CB-n-ir`. The full-order solution (solid line) acts as a reference. To avoid confusion, only a few frequencies are plotted for the reduced-order models. The numbers in the legend proceeding the reduction method denote the number of retained reduced interface modes, $N^{\boldsymbol{\Upsilon}}_{\mathrm{CB-ir}}$, for this model. For all reduced-order models, 40 fixed-interface normal modes are used. The lower plot in Fig. 6 shows the pressure FRF from the nodal force at point A to the hydraulic pressure at node B. It is found, that the reduced-order model `CB-ir-80` (black circles) and `CB-ir-40` (cyan plus signs) as well as the corresponding models `CB-n-ir-80` (red circles) and `CB-n-ir-40` (green plus signs) approx-

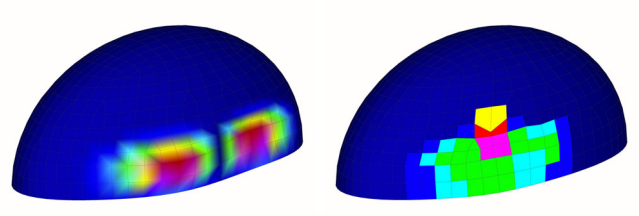

(a) Fixed-interface mode (b) Constraint mode

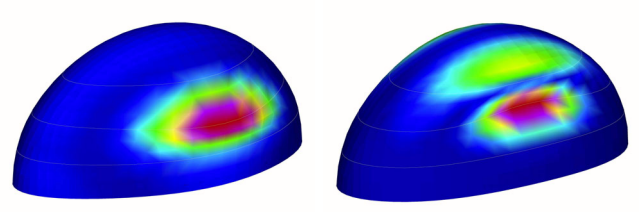

(c) Reduced interface mode (d) Reduced interface mode

Figure 4: Top: Fixed-interface normal modes and constraint modes for the classical Craig-Bampton method. Bottom: Reduced interface normal modes used for the method CB-ir and CB-n-ir.

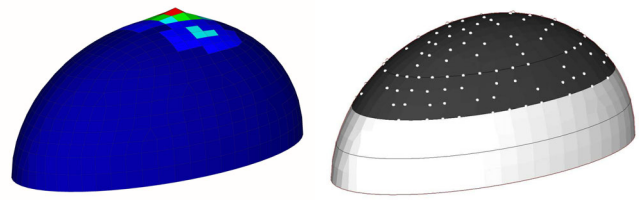

(a) (b)

Figure 5: Left: Attachment mode used for Rubin method. Right: Spots mark the selected attachment modes for method Ru-n-ir.

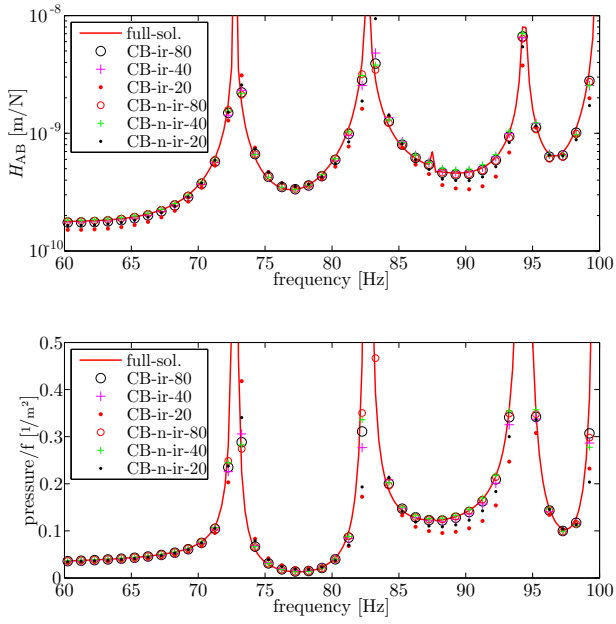

Figure 6: Dynamic compliance FRF and pressure FRF for the interface reduction methods CB-ir and CB-n-ir compared to full-order solution. All methods with 40 and more reduced interface modes approximate the transfer function very well.

imate both the dynamic compliance FRF and the pressure FRF accurately. It is worth noting, that for the classic Craig-Bampton method 1938 constraint modes would be used, opposed to 40 reduced interface modes for the models `CB-ir-40` and `CB-n-ir-40`. Thus, a significant reduction is obtained. If the number of retained reduced interface modes is further reduced, a loss off accuracy is observed. Both the model `CB-ir-20` (red points) and the model `CB-n-ir-20` (black points) show apparent differences for the dynamic compliance FRF and the pressure FRF.

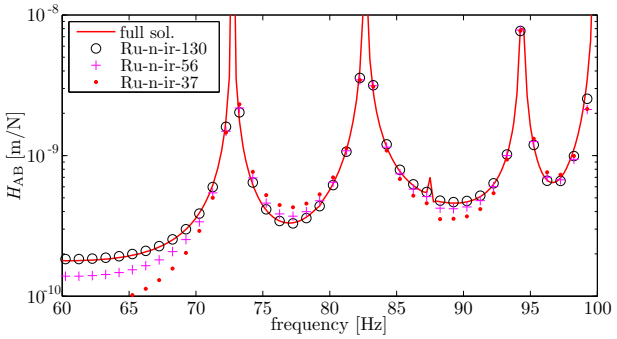

Figure 7: Dynamic compliance FRF for the interface reduction method Ru-n-ir compared to full-order solution.

Figure 7 depicts the dynamic compliance FRFs for the models obtained by the method `Ru-n-ir`. Again, the numbers in the legend denote the number of basis vectors in $\boldsymbol{\Upsilon}_{\mathrm{Ru}}$. With decreasing size of the reduction basis, the accuracy of the FRF also decreases. The model `Ru-n-ir-130` approximates the dynamic behavior with a good accuracy. The models `Ru-n-ir-56` and `Ru-n-ir-37` both show deviations for the low-frequency range. A further reduction in model size would lead to a less accurate representation of the FRF. This implies, that the use of the free-interface normal modes alone, as it is the case for model reduction by modal truncation, does not yield correct simulation results. Plots of the method `Ru-ir` are not presented in this work, since they show almost the same results and cause a higher computational cost during the reduction process. Concerning accuracy, for approximately the same size of the reduced-order model the methods `CB-ir` and `CB-n-ir` yield better results than the the method `Ru-n-ir`. This may be explained by the optimal selection of the subspace with respect to the strain energy norm for the Craig-Bampton based interface reduction methods.

Besides the accuracy, the computation times for the proposed methods plays an important role. The computation times are divided in two fields: The time needed for the coupled FE-BE solution and the time for the model reduction. Both proposed interface reduction methods show a significant acceleration of the FE-BE solution step. For example, the FE-BE solution at 72.00 Hz takes 1.6 s for the full-order solution on a Intel Xeon 5160 Processor and less than 0.1 s for all reduced order models. This acceleration is partly eaten up by the additional time needed for the model reduction. It takes between e.g. 8.6 s for the model `CB-n-ir-40`, 15.1 s for the model `Ru-n-ir-56` and 250 s for the model `CB-ir-80`. The overall speedup factor provides information about the real gain in computation time. It is defined as the ratio of the total simulation time of full-order model to the one of the reduced-order model. Hereby, the total simulation time is the computation of the frequency sweep including the time for the model reduction if applicable. A speedup factor of 8.6 for the model `Ru-n-ir-40` and of 7.8 for the model `Ru-n-ir-56` is measured. It is worth noting that both the classic Craig-Bampton and the classic Rubin method show a "negative" speedup of 0.7 and 0.6, respectively.

5 Conclusion

In this paper, two interface reduction methods are investigated, extending the range of the Craig Bampton and Rubin method to FE-BE coupled systems with a large fluid-structure interface. They are applied to simulate the low-frequency vibro-acoustic behavior of a partly immersed system. It is shown that the solution process is significantly accelerated while introducing only a small additional reduction error.

Acknowledgments

This research was financially supported by the Friedrich-und-Elisabeth-Boysen-Stiftung. The authors would like to acknowledge valuable contributions within the transfer project SFB404/T3 funded by the German Research Foundation (DFG).

References

[1] D. Brunner, M. Junge, and L. Gaul. A comparison of FE–BE coupling schemes for large scale problems with fluid–structure interaction. *International Journal for Numerical Methods in Engineering*, submitted for publication.

[2] R. R. Craig Jr. Coupling of substructures for dynamic analyses - An overview. In *AIAA/ASME/ASCE/AHS/ASC Structures, Structural Dynamics, and Materials Conference and Exhibit*, April, 3-6 2000.

[3] Etienne Balmès. Optimal Ritz Vectors for Component Mode Synthesis using the singular value decomposition. *AIAA Journal*, 34(6):1256–1260, 1996.

[4] M. K. Hakala. *Numerical modelling of fluid-structure and structure-structure interaction in ship vibration.* PhD thesis, Helsinki University of Technology, Espoo, Finnland, 1985.

[5] A.F. Seybert and B. Soenarko. Radiation and scattering of acoustic waves from bodies of arbitrary shape in a three-dimensional half space. *Transactions of the ASME*, 110:112–117, 1988.

[6] D. Brunner, M. Junge, C. Cabos, and L. Gaul. Vibroacoustic simulation of partly immersed bodies by a coupled fast BE–FE approach. In *Acoustics'08 Paris*, 29 June–4 July 2008.